Binding to the Ribosome by Eukaryotic Initiation Factor 4B Drives Yeast Translational Control in Response to Urea

Xiaozhuo Liu[1], Houtan Moshiri[1] and Sarah Walker[1,*]

[1] Department of Biological Sciences, SUNY at Buffalo, Buffalo, NY, 14260, US

* To whom correspondence should be addressed. Tel: 1-716-645-2272; Email: walker47@buffalo.edu

ABSTRACT

The yeast eukaryotic initiation factor 4B binds the 40S subunit in translation preinitiation complexes (PICs), promoting mRNA binding. Recent evidence suggests mRNAs have variable dependence on eIF4B, suggesting this factor could promote changes in mRNA selection to adapt to stressors. However, the importance of eIF4B and its constituent domains for mRNA selection under diverse cellular and environmental conditions remain undefined. Here we compared the effects of disrupting eIF4B RNA- and ribosome-binding under ~1400 growth conditions. The RNA-Recognition Motif (RRM) was dispensable for stress responses, but ribosome binding by the N-terminal Domain (NTD) promoted growth in response to various stressors. In particular, the NTD conferred a strong growth advantage in the presence of urea. Ribosome profiling revealed that the NTD promoted translation of mRNAs with long and highly structured 5-prime untranslated regions, both with and without urea exposure. Because these changes required 40S binding, our results suggest eIF4B regulates mRNA loading and scanning as a part of the PIC, rather than by activating mRNPs prior to ribosome binding. Furthermore, our data indicate the yeast response to urea includes a translational component, driven by translation of mRNAs encoding proteins associated with the cellular periphery, suggesting general eIFs can promote diverse cellular responses.

INTRODUCTION

Translation initiation begins with the formation of a translation preinitiation complex (PIC) comprised of an initiator Met-tRNA•eIF2•GTP ternary complex bound to the 40S ribosomal subunit along with eIFs 1, 1A, 5 and the multisubunit eIF3. Simultaneously, mRNAs are complexed with the eIF4F complex and Ded1/Ddx3, which are proposed to unwind secondary structure and promote PIC binding to mRNA. The eIF4F complex is comprised of eIF4E, which binds the 5'cap structure; eIF4G, a scaffold that binds to mRNAs, eIF4E, eIF4A, and other proteins; and eIF4A, a DEAD-box RNA helicase (1). This complex is thought to serve multiple purposes: 1) interactions of the 5'cap through eIF4E and other components of the PIC through eIF4G direct PIC loading to the 5'end of mRNAs and 2) helicase activity of eIF4A melts mRNA secondary structure near the cap and throughout the 5'UTR to allow effective loading at the cap and scanning through 5'UTRs. The associated protein eIF4B promotes the activity of the eIF4F complex in loading and scanning mRNAs (2,3). A number of observations indicate the importance of eIF4B in translating structured mRNAs and promoting the

activity of eIF4A/eIF4F both in vitro and in vivo (4-6). In fact eIF4B in yeast was first discovered by two groups as both a multicopy suppressor of a temperature-sensitive eIF4A mutation, as well as a protein that interacted with antibodies to the 5'-cap complex (7,8), indicating important functional interaction between eIF4F and eIF4B. One model for eIF4B is by enhancing eIF4A mRNA helicase activity to allow structured mRNA translation (2,9,10). However, recent work indicates that some classes of mRNAs have a hyperdependence on eIF4B while showing less dependence on eIF4G and/or eIF4A, suggesting eIF4B performs both eIF4A-dependent and eIF4A/eIF4F-independent activities during translation (6,11,12). These eIF4A-independent functions may stem from the ability of eIF4B to bind to the 40S subunit and promote conformational changes in the mRNA binding channel (6,13).

Yeast eIF4B can be divided into four functional domains: an N-terminal domain (NTD), an RNA-recognition motif (RRM), a 7-repeats domain, and a C-terminal domain (Figure 1A; (7,8). While the RRM has a defined globular structure with conserved RNA-binding motifs (14), the other three domains are predicted to be disordered (15). Our previous work demonstrated that eIF4B binds to the 40S subunit in a manner dependent on both the NTD and 7-repeats domains of the protein, and independently of the RRM (13). The 7-repeats domain consists of imperfect repetitions of a ~26 amino acid motif that can also bind directly to single-stranded RNA (7,8,13,16). Binding the 40S by either the NTD or 7-repeats domain promotes the movement of a ribosomal protein, Rps20/uS10 (13). This induces changes in the conformation of multiple residues on both the solvent and subunit interfaces of the 40S near domains of Rps20/uS10. Moreover, both the NTD and the 7-repeats domain of eIF4B are required for robust mRNA recruitment to the PIC, suggesting these ribosome binding activities are critical for translation. Deletion of either domain results in decreased rates of mRNA recruitment and translation in a manner that is partially rescued by increasing the concentration of eIF4B lacking the 7-repeats domain or overexpressing the protein. However, increasing concentrations the ∆ntd protein cannot (13). The increase in concentration of the ∆7-repeats mutant required for maximal rate could indicate that deletion of the repeats either directly disrupts a ribosome interaction needed for maximal affinity, or an interaction with another binding partner required for maximal activity. Deletion of the NTD, but not other eIF4B domains also confers a dominant-negative overexpression phenotype in cells harboring temperature-sensitive mutant eIF4F alleles, repressing growth even under permissive temperature (17). This suggests interaction of the 7 repeats with a binding partner sequesters a necessary function in the absence of the NTD. Deletion of either the NTD or 7-repeats domain increases the amount of eIF4A needed to achieve maximal rate of mRNA recruitment to the PIC, suggesting both domains are needed for optimal functional interaction of eIF4A with the preinitiation complex (13). Evidence was recently provided for direct interaction of the 7-repeats domain of eIF4B with eIF4A in vitro (18), and for interaction of eIF4B with eIF4F in vitro and in vivo to promote association of eIF4A with eIF4G (19). These observations together suggest a model in which the NTD of eIF4B binds to the 40S subunit, where it can effectively promote eIF4A activity on the PIC using the 7-repeats domain that can stabilize binding to the 40S subunit and enhance the conformational changes observed around Rps20/uS10.

In contrast to the ribosome binding activities of the NTD and the 7 repeats domains, disrupting the RNA-binding activity of the eIF4B RRM does not affect growth or translation activity in vitro or in vivo, unless combined with other mutations that affect function on their own, such as deletion of the NTD or 7-repeats (13). This suggests that the RNA-binding RRM can stimulate the required function of the NTD and 7 repeats, although to a limited extent which does not stimulate growth rate under standard laboratory conditions. The RRM is the only large functional domain with a large degree of conservation between yeast and human eIF4B (20), although there are small motifs of homology to the NTD and a segment of homology to the core sequence of a single yeast repeat just downstream of the RRM in the human factor that can rescue function of yeast eIF4B mutants lacking the analogous yeast motifs (17).

Here we investigated the role of the RNA-binding RRM and the 40S-binding NTD of eIF4B on translation and growth in response to stress conditions. We found that the NTD allowed enhanced growth in conditions that require robust cellular integrity, including media containing 3% w/v urea. Deletion of the NTD resulted in lack of eIF4B association with polysomes, and large decreases in translation that are exacerbated in the presence of urea. Analysis of the structural content of mRNAs that depend on the NTD supported the model that eIF4B is necessary to enhance translation of mRNAs with long, structured 5'UTRs that are less likely to form a closed-loop complex (6). Moreover, our data indicated that this ability of eIF4B requires NTD interaction with the ribosome. Because eIF4B ribosome binding is necessary for PIC transit through longer than average 5'UTRs, we conclude that eIF4B binding to ribosomal complexes enhances PIC scanning. The mRNAs that we observed had deficits in ribosome occupancy encode proteins associated with trafficking through and/or modification within the ER and Golgi network, suggesting their translation could reinforce the cellular periphery to respond to urea stress. Associated gene ontology classes for these mRNAs showed that proteins trafficked through the membrane system have inherently more structured 5'UTRs. This is expected to allow a high capacity for translational control of membrane proteins in response to various stressors that challenge cellular integrity. Together our data suggest eIF4B drives changes in translation of mRNAs encoding membrane and cell wall proteins to allow cells to adapt to diverse cellular environments.

MATERIAL AND METHODS

Construction of yeast strain and plasmids

Yeast strains YSW3 and YSW4 were generated by tetrad dissection of strain FJZ001 (*MATa/MATα, his3Δ1/his3Δ1 leu2Δ0/leu2Δ0 met15Δ0/MET15 LYS2/lys2Δ0 ura3Δ0/ura3Δ0 TIF3/ tif3Δ::hisG-URA3-hisG*) (13), followed by isolation of LYS+, HIS-, LEU-, and MET- haploid clones, and finally counterselection on 5-FOA for removal of the *URA3-HisG* cassette of the URA+ *tif3*Δ strain. TIF3 alleles with the native promoter and terminator encoding C-terminal hexahistidine tagged-eIF4B or variants were Gibson-cloned (NEB, USA) into the BamHI site of single-copy vector pHLUM (21) using

primers SW223/SW224 to amplify *TIF3-His6* with the native *TIF3* promoter and terminator from pFJZ056 for plasmid pSW150, *tif3Δntd-His6* from pFJZ141 to construct pSW151, and *tif3Δrrm-His6* from pFJZ140 for pSW152 (13). DNA sequences of the entire PCR-amplified regions were verified in the assembled plasmids. Sequences of cloning primers are as follows: SW223 (5'-GGC CGC TCT AGA ACT AGT GAC CTA ATT GAC ACC GTA C-3') and SW224 (5'-CGA CGT AGT CGA GGA TCG CTT CTT CTT TTG AAT ATT ACC-3'). Plasmids pSW150, pSW151, and pSW152 were transformed into YSW4 (*MATa, his3Δ1, leu2Δ0, ura3Δ0, met15Δ0, tif3Δ0*) to generate prototrophic strains YSW5, 6, and 7 expressing WT, Δntd, and Δrrm eIF4B alleles, respectively. Transformed strains were verified by Western blot for correct eIF4B variant expression (Figure 2D).

Phenotyping Experiments

Previous work showed that inclusion on the same plasmid of the four requisite metabolic genes lacking in the parental genome of the barcoded yeast knockout collection (*HIS3*, *LEU2*, *URA3*, and *MET17*) provided a selective growth advantage, regardless of whether the metabolites these genes produce were included in the media. Hence, the plasmid with four metabolic markers is effectively retained even in rich growth media without selection, and synthetic growth effects between metabolic gene deletion and the mutation of interest can be avoided (21). Prototrophic strains YSW5, 6, and 7 were sent to Biolog for Phenotype Microarray screening at 30°C in duplicate, using plates 1-10 and 20-25 (Biolog Inc, USA) (22). Plates were read every 30 minutes for 48 hours.

Yeast Growth

Yeast were cultivated in liquid or on solid (2% agar) Synthetic Drop-out (SD) media (20 g/L glucose, 1.71 g/L yeast nitrogen base without amino acids, 5 g/L ammonium sulfate; Sunrise Scientific Products, USA) at 30°C. For assays with additives, yeast cells from an overnight culture in SD media were diluted to an OD_{600} of 0.05 in SD media or SD media supplemented with additive (e.g. 2% or 3% urea), and allowed to grow to mid-log phase with vigorous shaking at 30°C, unless otherwise noted. Automated growth curves were performed in 96-well plates (200 µl SD per well) by taking OD_{600} measurements every two hours for 48 hours while incubating at 30°C with double-orbital shaking in a Spark plate reader (Tecan, Switzerland).

Analysis of Polysome:Monosome ratios

Polysome profile analysis was performed as described previously (13,23). For figure 2C and Fig S1D, yeast cells were cultured in SD medium with or without additives as noted at 30°C to an OD_{600} of 1.5. Cycloheximide (Gold biotechnology, USA) was added to a final concentration of 50 µg/ml and incubated for 5 minutes at 30°C with shaking before collecting cells by pelleting in centrifuge bottles packed with ice. Pellets were resuspended in 1/3 of the pellet weight of breaking buffer (20 mM Tris-HCl at pH 7.5, 50 mM KCl, 10 mM MgCl2, 1 mM DTT, 200 µg/mL heparin, 50 µg/mL cycloheximide, and 1 Complete EDTA-free Protease Inhibitor Tablet [Roche]/50 mL buffer), dropped into liquid nitrogen, and lysed in a Nitrogen Mill for 10 Cycles following a precool of 15 minutes with the following parameters: 1 minute run, 2 minutes cool, rate=15 (Spex Sample Prep, USA). 25 A_{260} units

of lysates were resuspended in 1.5 volumes of the pellet weight of ice-cold breaking buffer and clarified by spinning at 14,000 rpm for 15 minutes at 4°C prior to separation by velocity sedimentation on 5-45% sucrose gradients (20 mM Tris-HCl [pH 7.5], 50 mM KCl,10 mM $MgCl_2$,1 mM DTT, 5-45% sucrose) by centrifugation at 39,000 rpm for 2.5 h at 4°C in a Beckman SW41 rotor. Gradient fractions were separated on a gradient station (BioComp, Canada) while scanning at 254 nm. The areas under the monosome and polysome peaks, determined in GraphPad Prism software, were used to calculate the P/M ratio.

Western analysis

To verify that eIF4B variants were expressed under stress, yeast cells were grown in SD media with or without 2% or 3% urea, and harvested at an OD_{600} of 1.0. Whole cell extracts (WCEs) were prepared by extraction with trichloroacetic acid (TCA) and subjected to Western blot analysis as described previously (13) using antibody against the His6 epitope (EMD Millipore 70796.) For analysis of eIF4B position within gradients, 0.5 ml of each gradient fraction used for qRT-PCR below was precipitated by addition of 0.05 ml 100% (w/v) TCA and spinning for 10 minutes at 12,000 x g, resuspended in SDS loading buffer, and resolved by SDS-PAGE, followed by Western blotting using anti-His antibody. Each experiment was repeated at least two times.

RiboSeq and RNASeq library preparation

Ribosome footprint profiling was conducted as described (24-26) with minor modifications. Yeast cells at an OD_{600} of approximately 0.8 were rapidly harvested by vacuum filtration through a 0.45 µm Whatman cellulose nitrate membrane filter (GE Healthcare Life Sciences, USA) at room temperature by scraping the slurry into liquid nitrogen. Cells were lysed as above in a Nitrogen mill, and thawed and suspended in lysis buffer (20 mM Tris [pH 8], 140 mM KCl, 1.5 mM $MgCl_2$, 1% Triton X-100, 100 µg/ml cycloheximide). 25 A_{260} units of extract were treated with 87.5 Units of RNase If (M0243, NEB, USA) for 1h at 22°C on a rotator, then separated on 10-50% sucrose gradients (20 mM Tris [pH 8], 140 mM KCl, 1.5 mM $MgCl_2$, 1mM DTT, 100 µg/ml cycloheximide, 10-50% sucrose) by centrifugation at 40,000 rpm for 3 hours at 4°C in a Beckman SW41 rotor and fractionated as above. Ribosome-protected mRNA footprints were purified from the nuclease-treated monosome fraction by addition of SDS to 0.8% at 65°C, followed by extraction with acid phenol [pH 4.5] (Ambion, USA) and then chloroform/isoamyl alcohol extraction. 300 mM NaOAc [pH 5.2] was added to the aqueous phase and RNA was precipitated with one volume of isopropanol before resuspending in 10 mM Tris-HCl [pH 8]. RNA footprints from 25 to 35 nt were size-selected on a 15% denaturing PAGE gel, eluted by crushing and soaking gel fragments in RNA elution buffer (300 mM NaOAc [pH 5.5], 1 mM EDTA, 0.1 U/µl SUPERaseIn (Life Technologies, USA)), and dephosphorylated using T4 Polynucleotide Kinase (M0201, NEB, USA) prior to isopropanol precipitation and resuspension in 10 mM Tris [pH8]). A pre-adenylated universal linker (5'-rAppCTGTAGGCACCATCAAT-NH_2-3') was prepared in house or purchased from NEB (S1315S) and ligated to the 3' ends of the dephosphorylated footprints using T4 RNA Ligase 2, truncated (NEB, MO242L). rRNA was depleted using the Yeast Ribo-Zero Gold rRNA removal kit (Illumina, USA). First strand synthesis was performed with Superscript III (Life

Technologies, USA) and reverse transcription primer NINI9 (5'-/5Phos/ AGA TCG GAA GAG CGT CGT GTA G GGA AAG AGT GTA GAT CTC GGT GGT CGC /SpacerC18/ CAC TCA /SpacerC18/ TTC AGA CGT GTG CTC TTC CGA TCT ATT GAT GGT GCC TAC AG), followed by circularization with Circligase (Epicenter, USA). Circularized cDNA was then PCR amplified using primer NINI2 (AAT GAT ACG GCG ACC ACC GAG ATC TAC AC) and a primer with a barcode (CAA GCA GAA GAC GGC ATA CGA GAT XXX XXX GTG ACT GGA GTT CAG ACG TGT GCT CTT CCG), where XXXXXX denotes a six-nucleotide-barcode used to distinguish samples run in the same lane (Table S1). For RNA-seq, total RNA was isolated from the same cell extracts using SDS/hot acid phenol/chloroform extraction. The Ribo-Zero Gold Yeast kit was used to remove rRNA, and total RNA was randomly fragmented by incubating for 20 minutes at 95°C in freshly made fragmentation buffer (100 mM sodium carbonate-bicarbonate [pH 9.2], 2 mM EDTA). RNA was then precipitated and fragments of 40–60 nt were purified from a denaturing PAGE gel, and library generation carried out as above. Ribo-Seq and RNA-Seq were performed for two independent cultures for each condition (WT and Δntd cells grown in SD both with and without 3% Urea), and the 16 libraries sequenced in 2 lanes with 150 bp reads on an Illumina HiSeq 4000 instrument by Genewiz, USA.

Analysis of ribosome profiling libraries

The Ribogalaxy platform (https://ribogalaxy.ucc.ie, (27)) was used for trimming linker sequences (Cutadapt version 1.1.a; (28)), subtractive alignment of *S. cerevisiae* non-coding RNAs (Bowtie version 1.1.a; (29) using the R64.2.1 S288C genome from Saccharomyces Genome Database (SGD, RefSeq ID: 285498), alignment of rRNA subtracted libraries to the transcriptome (Bowtie version 0.1.3 using the SGD transcriptome dataset and counting of uniquely mapped reads (24) using Ribocount version 0.3.1. Statistical analyses of differences in total RNA counts, ribosome footprints, or TE values between WT, mutant, urea-treated, and untreated samples were conducted using DESeq2 (30). Gene ontology categorization of library-specific differences was performed at SGD.

qRT-PCR

Cell lysates were prepared and 12 fractions were collected from polysomes fractionated using the protocol for riboseq gradient preparation above (without nuclease treatment), and the remaining fraction was used for Western analysis. 0.3 ml of each gradient fraction was spiked with equal amounts of control RNA (Fluc mRNA, Trilink Biotechnologies, USA), then total RNA was extracted using the hot acid phenol-chloroform method (31). First strand synthesis was performed with iScript Advanced Reverse Transcriptase (Biorad, USA) using oligo-dT primers and random hexamer primers. Quantitative PCR was performed with iQ SYBR Supermix reagents (Biorad, USA) using CFX384 Touch Real-Time PCR detection system (Biorad, USA) two times per sample. Gene-specific primer sequences are: ACT1/YFL039C (CGT CTG GAT TGG TGG TTC TAT C, GGA CCA CTT TCG TCG TAT TCT T); ADH4/YGL256W (TGC TGTC AAC GAT CCA TCT AC, AGA GGC GGT GGA AAC ATA AG); AGA1/YNR044W (GTA AGT GAA GCC ACG AGT ACA T; CAG ACA AGG AGG AGG ATG AAA G); AGA2/YGL032C (GAA TCG ACG CCG TAC TCT TT, GGG TGA GAA CCG CAA TTA CT); FIG2/YCR089W (GCA GTG TTG ACA GGT TTG TTT; CTT ATG GTG GTG GTA GCA GTA G);

FLUC (TCA TCA TGG ACA GCA AGA CC, CAC GAA GTC GTA CTC GTT GAA); GCN4/YEL009C (CCA GTT ACC ACT GAC GAT GTT, AGT TGT CGA GAC TTC CAG ATT G); VBA2/YBR293W (CCG AAC TGG TTG ATT GGT CTA T, GCA GTA GCT TGG TCA CTC TTA G); YER186C (GTT TAC CAG AGG TGG GTG ATA G, CCT CCT TAG TTC TGC ACA TAC A); YOR015W (GCA TAC TTC AAT CGA TGT GTC TTC; AAA TAG AGG AAA GGC AGA AGG AA).

RESULTS

The N-terminal domain of eIF4B promotes translation and association with polysomes in vivo

Previous work demonstrated that the N-terminal domain (NTD) of eIF4B promotes both association with the ribosome in vitro and translation in vivo, while the RRM of eIF4B is dispensable in auxotrophic yeast strains. Given the diverse dependencies of cellular mRNAs on eIF4B function, we thought it likely that differential mRNA selection could confer phenotypic advantages. We wondered if the ability of the NTD to promote translation would afford cells the ability to resist different stressors, and whether the RRM would provide additional function under stress, so we constructed prototrophic strains for phenotype microarray analysis. It has previously been noted that synthetic effects can arise from metabolic marker deletions and various gene deletions in the barcoded yeast knockout collection, even when the nutrient for which that gene is needed was provided exogenously (21). To eliminate the possibility of similar synthetic phenotypic effects and to simplify growth and analysis, an eIF4B null mutant was transformed with a plasmid that complemented the four existing auxotrophic markers and provided a WT, ∆rrm, or ∆ntd eIF4B gene copy (*TIF3, tif3 ∆rrm,* or *tif3 ∆ntd*) under the native promoter and terminator (Figure 1A., S1A) Separation of cellular lysates on sucrose gradients in the presence of cycloheximide (to stall translation elongation) allows quantification of ribosomes bound per mRNA in cells, a measure of translation initiation efficiency. Polysome profiles from prototrophic strains expressing WT or ∆ntd eIF4B confirmed that the NTD deletion led to a gross reduction of polysomes and an increase in monosomes in the mutant (Figure 1B, C), indicating the NTD promotes global translation initiation in vivo in a prototrophic background. In addition, immunoblotting gradient fractions for a C-terminal His-tag on eIF4B indicated the presence of eIF4B in 40S and polysome peaks in vivo (Figure 1B). The amount of eIF4B associated with ribosome and polysome fractions was greatly reduced by deletion of the N-terminus (Figure 1C). Residual association of eIF4B ∆ntd with fractions containing ribosomes was apparent and could be explained by interaction of the 7-repeats domain that also contributes to 40S binding (13), by weakened association of the ∆ntd protein followed by dissociation, or by association of the ∆ntd protein with larger mRNPs that comigrate with the 40S. We also observed a large amount of both WT and ∆ntd eIF4B in the mRNP fraction. Lysates were not treated with formaldehyde prior to loading on gradients, so it is expected that some portion of initially ribosome-associated factors would dissociate and be observed in the upper regions of the gradient. The large amount of WT eIF4B in the upper gradient fractions may thus be attributed to dissociation of the protein from the 40S or preinitiation complex upon dilution within the gradient, or due to association of some of the eIF4B with mRNA in the cell. Nevertheless, it is clear that deletion of the NTD greatly reduces both eIF4B association with ribosomes and polysomes, and ribosome association with mRNA.

The NTD of eIF4B promotes translation-mediated stress responses

To determine conditions under which the NTD of eIF4B plays a specific role in regulating translation, we performed phenotype microarrays of cells expressing WT or ∆ntd eIF4B from a single copy plasmid that also restored nutrient prototrophy. Phenotype microarray analysis showed a large number of conditions in which the prototrophic ∆ntd eIF4B expressing strain grew at a reduced rate compared to the wild-type eIF4B expressing cells (Figure 2A). The strongest responses (Table S2) include osmolytes, detergents, a number of peptides as nitrogen sources, and antibiotics. Urea, which gave the strongest negative phenotype when present at 3% w/v in the media, acts as a denaturing agent and can cause membrane blebbing at high concentrations (32,33), and can readily cross the yeast cell wall and membrane to act as a nitrogen source (34). Tamoxifen, which targets the estrogen receptor in higher eukaryotes, targets the calmodulin protein in yeast which regulates stress responses through Hog1 interaction (35,36). Poly-L-Lysine can act as a cationic detergent or a charged adherent for various molecules, and likely interacts with the cell wall or membrane. The strain lacking the NTD of eIF4B also showed heightened sensitivity to antibiotics that target the small ribosomal subunit, apramycin sulfate and to a lesser extent tobramycin. WT yeast are not sensitive to these antibiotics, which when combined with the sensitivity to various salts (Potassium chloride, Chromium chloride, and to a lesser extent, sodium chloride) and other phenotypes described above, suggests a defect in membrane and/or cell wall permeability in the mutant. Growth defects were verified for ∆ntd-expressing cells in the presence of urea, which conferred the largest reduction in the mutant (Figure 2B). These experiments demonstrated that WT growth rate is unaffected by urea while the mutant shows slow growth. Together the results suggest interactions of the eIF4B 40S-binding NTD allow resistance to a number of growth conditions that challenge cellular integrity, and that the mutant may have a defect in membrane and/or cell wall permeability. In contrast, deletion of the RNA-binding RRM domain conferred no large reproducible advantage or hindrance, suggesting the RNA-binding activity of eIF4B is dispensable for growth in all conditions tested (Fig S1).

To further investigate the mechanisms by which the NTD promotes growth in the presence of stressors, we compared polysome traces for WT and ∆ntd eIF4B-expressing cells grown in the presence and absence of 2% or 3% urea (Figure 2C). Whereas WT eIF4B-containing cells showed little to no decrease in polysome to monosome (P:M) ratio in either concentration of urea, ∆ntd cells showed a further 36% and 50% decrease in P:M ratio due to urea exposure. This change in translation is not due to decreased levels of eIF4B, as immunoblotting for a His tag on the eIF4B C-terminus shows similar protein levels in each strain when grown in media with varied urea concentrations (Figure 2C). Together these data suggest eIF4B binding to the ribosome by the NTD allows robust translation in the presence of urea.

The eIF4B NTD promotes translation of mRNAs associated with the cellular membrane

We next performed ribosome profiling on the yeast cells expressing WT or ∆ntd eIF4B both with and without urea to determine the mechanism by which eIF4B•40S leads to changes in translation of individual mRNAs. We prepared illumina-indexed cDNA libraries for RNAseq and Riboseq from WT

and Δntd eIF4B-expressing cells in the presence or absence of 3% urea. Comparison of replicates indicates sufficient reproducibility for each sample, with slightly higher variability in the Riboseq libraries from Δntd eIF4B-expressing cells with 3% urea (Figure S2), which showed the strongest global repression of translation and therefore had the least ribosome footprints. After mapping and quantifying footprints on mRNAs in the yeast transcriptome, we compared the averaged changes in RNAseq, Riboseq, and TE (translation efficiency, Riboseq/RNAseq) in response to urea exposure in WT versus the urea-dependent change in Δntd eIF4B-expressing cells (Figure 3, Table S3). Changes in individual mRNA levels in response to urea were more similar between the two strains (Figure 3A, r=0.622), while changes in ribosome footprints and changes in TE for individual mRNAs in response to urea showed less correlation between the two strains (Figure 3B, C; Riboseq, r=0.361; TE, r=0.156). This is further evidenced by evaluation of the mRNAs with ≥ 1.5-fold increase in RNAseq, Riboseq and TE in response to urea. While there were fewer mRNAs showing ≥1.5-fold urea-dependent increases in RNA levels (Figure 3D; WT= 39, Δntd=108)) with substantial overlap between the WT and mutant pools (43.5% of mRNAs showing ≥1.5-fold decrease for WT eIF4B cells also increased by ≥1.5-fold in Δntd), there were large numbers of mRNAs with ≥1.5-fold changes in RiboSeq (Figure 3E, WT=141 mRNAs, Δntd=543 mRNAs) and TE (Figure 3F, WT=300 mRNAs, Δntd=163 mRNAs), both in the WT and Δntd eIF4B-expressing cells. Moreover, the pools of mRNAs showing changes in TE upon exposure to urea were almost completely distinct in the control cells versus the mutant. It is important to note that while there are a greater number of individual mRNAs showing a relative increase in Riboseq in the mutant in response to urea, these cells show an overall decrease in global translation initiation as evidenced by decreased P:M ratio (Figure 1C, 2C). Changes in ribosome occupancy of representative mRNAs were verified by performing qRT-PCR on gradient fractions from cells expressing WT and Δntd eIF4B in the presence and absence of 3% urea in the growth media. The trends observed by ribosome profiling are confirmed by this independent method for several representative mRNAs in each pool (Figure S3). These data indicate that the eIF4B•40S binding NTD promotes changes in growth by differentially affecting translation of specific mRNAs in response to stress.

To understand how eIF4B NTD-dependent changes in translation promote growth in urea, we performed gene ontology analysis of the RNAs ≥1.5-fold increased or decreased TE in response to urea in WT or mutant cells (Figure 3G). Of the 210 mRNAs with ≥1.5-fold increased translation in WT cells upon exposure to urea, 102 mRNAs were associated with the parental membrane term, while significant numbers of mRNAs were associated with the cell wall, cellular periphery, and other related terms, suggesting eIF4B•40S association leads to enhanced translation of mRNAs encoding proteins that remodel the cellular membrane. In contrast, of 163 mRNAs showing ≥1.5-fold increased translation in Δntd-expressing cells in response to urea, 151 were associated with the cytoplasm gene ontology term (Table S4). Likewise, analysis of the mRNAs showing increased TE in Δntd cells showed strong association with GO terms for ribosomes and cytosolic components, even without urea (Table S5). Furthermore, mRNAs that showed decreased translation when the eIF4B NTD was

removed in the absence of urea were associated with membrane-bounded organelles (Table S6). This suggests the NTD promotes translation of mRNAs encoding membrane-associated proteins, and the loss of this ability results in the mutant translating mRNAs that encode cytoplasmic proteins, leading to urea and other stress sensitivities. Finally, we analysed the 281 mRNAs showing more than 1.5-fold decreased translation efficiency in response to urea in the mutant cells relative to WT. In this case we saw decreased translation for 84 mRNAs associated with the endomembrane system (p-value=0.000026), including association with the ER, Golgi, and transferase activities, glycosylation and mannosylation (Table 1). This suggests effective translation of mRNAs for proteins trafficked through the ER/Golgi network to the membrane and cell wall is dependent on eIF4B binding to the ribosome. Interestingly, the specific mRNAs that were hyperdependent on the eIF4B NTD showed little overlap with those mRNAs identified as hyperdependent on eIF4B when analysing the translatome of an eIF4B null mutant (data not shown,(6) despite sharing general structural features discussed below. However, in the previous analysis of cells lacking eIF4B, cells were shifted to 37°C for 2 hours prior to ribosome profiling, so differences in translation of individual mRNAs could also be due to this variable. Together these results suggest that eIF4B•40S binding is necessary for critical changes in translation of RNAs that remodel the cellular periphery in response to urea exposure. This function is necessary for translation of the optimal pool of mRNAs to promote rapid growth in standard media as well.

The NTD of eIF4B promotes translation of mRNAs with long and structured 5'UTRs

Previous studies have shown that mammalian eIF4B is necessary for PIC assembly at the start codon of mRNAs with 5'UTR secondary structure in vitro (4). Likewise, yeast eIF4B is associated with robust loading and scanning of PICs and translation of mRNAs and synthetic reporters containing higher than average secondary structure in vitro and in vivo (5,6). We speculated that the effect of eIF4B ribosome binding on translation of mRNAs needed to combat extracellular urea is related to the ability of eIF4B to promote translation of structured mRNAs. To test this hypothesis, we analysed available parallel analysis of RNA structure (PARS) scores (37) for the mRNAs exhibiting changes in translation as a result of eIF4B NTD deletion, in the presence or absence of urea. PARS scores provide the relative propensity of each nucleotide to a single- or double-strand specific nuclease, with a higher PARS score indicating a higher propensity for secondary structure. Cumulative PARS scores can be compared for specific regions of mRNAs to determine the likelihood that the e.g. first 30 nucleotides, total 5' UTR, or regions in the ORF have more structure (Figure 4A), which would present an impediment for PIC loading, PIC scanning, or translation elongation respectively (6). We found that deletion of eIF4B led to lower translation efficiency (≥1.5-fold decrease) of mRNAs with significantly higher PARS scores for the first 30 nucleotides of the 5'UTR. An even larger difference was observed for the total 5'UTR, suggesting interaction of the eIF4B NTD with the 40S promotes effective mRNA loading and possibly scanning through structured mRNA 5'UTRs (Figure 4B). The average individual nucleotide PARS score averaged for the full 5'UTRs was likewise significantly higher for these groups of mRNAs that were hyperdependent on the eIF4B NTD for translation (Figure 4C). In contrast, there was not a significant change in the PARS scores for the 30 nucleotides surrounding the start codon,

or the first 30 nucleotides of the ORF, suggesting structure around the start site and in the ORF does not strongly require eIF4B activity. In fact, the PARS scores for the Plus45, Plus60 and Plus75 regions were significantly lower for the group of mRNAs that were hyperdependent on the NTD of eIF4B (in the absence of urea). This suggests that the eIF4B NTD is not required for translation of structured ORFs or structured RNAs in general, but instead is important for PIC loading and movement through structured 5'UTRs (Figure 4A, B). The mean length of 5'UTR was also significantly higher for the group of mRNAs that were less efficiently translated (≥1.5-fold) when the NTD of eIF4B was deleted. This further suggests interaction of the NTD with the 40S is critical for effective scanning of long structured 5'UTRs (Figure 4D). This effect was more pronounced when cells were grown in the presence of 3% urea prior to ribosome profiling, suggesting the effect of eIF4B•ribosome binding on urea resistance stems from the ability of eIF4B to promote effective scanning when attached to the PIC.

We also found that 155 mRNAs showed a relative increase in translation in ∆ntd cells (Figure 3F), indicating ribosomes were able to be loaded on these mRNAs without eIF4B bound. We assessed the degree of secondary structure in the 5'UTRs and coding sequences of these mRNAs (Figure S4). It was previously shown that mRNAs that were translated relatively more efficiently in an eIF4B null mutant showed increased association with components of the closed loop complex (6): eIF4E, eIF4G and PABP (38). We compared mRNAs classified as strong-closed loop potential (higher association with closed-loop components) and no closed-loop (enriched in inhibitors of the closed-loop complex(38)) to mRNAs that were translated ≥1.5-fold more efficiently in the ∆*ntd* mutant. We found that mRNAs that showed increased translation in ∆ntd (with or without urea) showed similar trends with respect to PARS scores as those mRNAs defined as having strong closed-loop potential, and the opposite behavior as those mRNAs defined as having no closed-loop potential. Both the cumulative 5'UTR regions and the average nucleotide PARS scores for the 5'UTRs of these mRNAs were lower than the average yeast mRNA. In contrast, the mRNAs that showed increased translation efficiency in the ∆ntd mutant and strong-closed-loop associated mRNAs were more structured than the average yeast mRNA in the ORF. This suggests that mRNAs that rely on closed-loop components for mRNA loading do not require eIF4B binding to the ribosome, and reinforces the conclusions of the previous manuscript that mRNAs requiring eIF4B activity are less associated with closed-loop components (6).

RNAs encoding proteins trafficked through the ER and Golgi have long structured 5'UTRs, imposing a heightened requirement for eIF4B

Phenotype microarray analysis suggested the NTD of eIF4B promoted growth in a number of conditions that challenge cellular integrity (Figure 2A, Table S2). The findings that mRNAs translated more effectively by eIF4B containing the NTD had longer and more structured 5'-untranslated regions led us to question whether the entire GO term classes of mRNAs that were overrepresented in our analysis are inherently more structured. If true, this would be expected to impose regulatory capacity as cells encounter stresses that require membrane changes, and may explain how the NTD of eIF4B affords resistance to diverse stressors that may require different membrane composition. We then compared the PARS scores for all yeast mRNAs versus the PARS scores for all yeast mRNAs

associated with GO terms for mRNAs that required eIF4B for translation in response to urea. This group includes: intrinsic component of the membrane (the GO term with the lowest P value for association with RNAs showing increased translation in response to urea in WT cells); as well as transferase activity, endomembrane system, glycosylation, and mannosylation (the parent GO terms associated with mRNAs with decreased translation in response to urea in the mutant cells.) Interestingly, we found that the 5'UTRs of mRNAs associated with each of these GO terms had higher average Total PARS scores than the average yeast mRNA (Figure 4E). However, only those mRNAs encoding intrinsic components of the membrane had significantly longer 5'UTRs (Figure 4F). The mean 5'UTR PARS scores for individual nucleotides was also significantly higher than the average yeast mRNA for all classes (Figure 4G), indicating these classes of mRNAs have inherently more structure in the 5'UTR. This suggests functional importance of structural elements in regulating translation of membrane-associated and trafficked proteins.

DISCUSSION

In this study, we characterized the contribution of eIF4B RNA- and 40S subunit-binding activities to translation regulation as well as the ability to promote adaptation of yeast to diverse stressors. We found that the NTD of eIF4B promoted association of eIF4B with translating ribosomes in vivo while allowing translation of mRNAs with longer than average and highly structured 5'UTRs.The NTD also afforded yeast the ability to translate mRNAs encoding proteins trafficked through and modified in the ER and Golgi to reside in cellular membranes. These proteins are expected to reinforce the cellular periphery and allow yeast to cope with external stressors.

The RRM of eIF4B was thought to promote mRNA recruitment to ribosomes by providing an RNA anchoring point on a ribosome or eIF3-bound molecule (namely for mammalian eIF4B, (39-42)) or by promoting RNA strand-exchange activities of eIF4B (16). Our previous work suggested that instead, the RNA-binding activities of the RRM are dispensable for eIF4B function in yeast (13). However, because the experiments in our previous work analysed the function of Δrrm-expressing eIF4B under optimal growth conditions, it remained plausible that the RRM provides additional functions to cells under stress, when additional interactions may be needed to direct ribosomes to specific mRNAs. Our Biolog analysis of the Δ*rrm* mutant provides strong evidence that the RRM domain is in fact dispensable for function of this protein in yeast, at least in liquid media. The only plate in which we saw mild phenotypes for the Δ*rrm* mutant was in the presence of certain alternative sulfur sources (Figure S1), but the changes observed were well below the cutoff for significance and were not reproducible. It remains possible that survival in non-vegetative differentiated states could depend on the RRM, and this may explain why the RRM is more important in multicellular organisms (41,42). Alternatively, the contribution of the RRM to cellular survival may not be sufficient to detect a change in growth rate or cellular fitness, but could allow RRM-containing yeast to outcompete mutants defective in RNA-binding. This could have led to retention of the RRM over the course of evolution (8).

In contrast to yeast lacking the eIF4B RRM, we found that yeast lacking the NTD were highly sensitive to a number of conditions that WT cells are able to tolerate, and that these effects were mediated through changes in translation (Figure 2). The mRNAs that showed decreased translation efficiency when the NTD was lacking had a number of features similar to what was observed for an eIF4B null strain. The 5'UTRs of these mRNAs were longer and more structured than the average yeast mRNA (Figure 4), reinforcing many observations that eIF4B promotes translation of structured mRNAs (2,4,6,10). The mechanism by which eIF4B is proposed to promote translation of these mRNAs resides in its ability to interact with eIF4A and stimulate helicase activity. However, a report for direct interaction of these factors suggests that the 7-repeats domain of eIF4B binds eIF4A (18). In our study, we observed decreased translation of structured mRNAs when we disrupt eIF4B•40S binding by the NTD. This suggests that the mechanism for eIF4B stimulation of structured mRNA translation resides at least to some extent in its ability to bind the ribosome (Figure 5). We have also previously reported defects in functional interaction of eIF4A and eIF4B when either the 7 repeats or the NTD is deleted, and observed that overexpression of ∆ntd has a dominant negative effect on an eIF4A mutant (13,17). Together these observations could indicate that deletion of the eIF4B NTD may sequester eIF4A in an inactive state off of the ribosome and/or prevent a PIC conformation required for optimal scanning. In either case, our data suggest eIF4B mediates effective scanning through long structured 5'UTRs by binding to the ribosome.

The strongest NTD-specific defect was observed in the presence of urea, which had no effect on WT growth rate or translation (P:M ratio) at concentrations that strongly repressed growth and translation of the mutant (Figure 2A-C). Urea affects several processes in *S. cerevisiae*, where it can serve as a nitrogen source, have effects on the membrane, and can denature structured nucleic acids. At the concentrations used here, it was reported that urea can readily cross the cellular membrane (34), presumably via the Dur3 transporter (43), and be used as a nitrogen source. Membrane blebbing and denaturation of nucleic acids is unlikely to occur at the ~0.5M urea used here for ribosome profiling (32,33). It is possible that gene expression changes are responsible for resistance at this level of urea, but upon deletion of eIF4B, the normal translation program is disrupted leading to sensitivity. Our RNASeq analysis indicates that in response to urea, there is a ~4-fold increase in DUR3 mRNA in WT cells, and a ~3-fold RNA increase in ∆ntd-expressing cells, suggesting a transcription-program or RNA stability difference (independent of eIF4B activity) is activated upon urea exposure, which leads to higher levels of *DUR3* mRNA. However, the *DUR3* mRNA is also dependent on the NTD for translation in urea, showing a 1.6-fold decreased TE in urea when the NTD was deleted relative to WT TE in urea (Table S3). It is possible that eIF4B-dependent translation of transmembrane urea transporters such as Dur3 can fine-tune the amount of urea imported or exported from the cells.

While most fungi use urease as a virulence factor and to break down urea, the Saccharomycetes (including *Saccharomyces, Candida*, and other genera) lack urease genes and instead use the

Dur1,2 amidoylase to break down urea into ammonia and carbon dioxide in a biotin-dependent, two-step process (43,44). Our ribosome profiling data indicated that the *DUR1,2* mRNA was present at ~4-fold higher levels in both WT and mutant cells in response to urea (Table S3), but that the mRNA was translated ~1.5-fold less efficiently in urea when the NTD is deleted, indicating eIF4B-independent RNA control and eIF4B-dependent translational control of gene expression. Dur1,2 was demonstrated to be necessary for Candida differentiation and escape from macrophages during infection (45). There is very little sequence conservation between the NTD of yeast and human eIF4B, but these domains are well-conserved in *Saccharomyces* and *Candida* species. Because the *Saccharomyces* NTD deletion leads to changes in *DUR1,2* expression, the NTD of eIF4B could be a putative target for combating *Candida* infections.

Gene ontology analysis of ≥1.5-fold translation efficiency changes indicated that mRNAs encoding proteins associated with the membrane, and to a lesser extent cell wall, were translated at higher levels in WT cells in response to urea (Figure 3). Likewise, mRNAs encoding proteins associated with endomembrane system and modifications that arise within the ER and Golgi were unable to be translated efficiently in response to urea in the mutant cells (Figure 3, Table 1). The resulting membrane proteins are involved in a number of cellular processes. For instance, several proteins associated with adhesion during a-cell mating (Fig1, Fig2, Aga1, and Aga2; Table S3; Figure S3) showed TE changes in cells lacking the eIF4B NTD (decreases in TE in urea of 30-, 8-, 6- and 4-fold, respectively when compared to WT TE in urea). Recent analyses of uORF usage of yeast cells exposed to temperature shifts indicated that *AGA1* and *AGA2* showed changes in uORF usage in response to temperature shifts. In the presence or urea, or in response to NTD deletion we do not see changes in uORF usage of the *AGA2* mRNA. We do not see usage of the *AGA1* uORF in any of these experiments, suggesting the uORF occupancy observed in the former study was specific to changes in start codon fidelity in the high temperature response.

DATA AVAILABILITY

Raw sequencing reads and alignment files have been deposited in GEO with accession number GSE139097.

ACKNOWLEDGEMENTS

The authors would like to thank Fujun Zhou for assistance generating yeast strains; Alan Hinnebusch and Jon Lorsch for providing reagents; Mary Thompson, Audrey Michel, Onta Lin, Marie Saitou, Zhe

Ji, and Michael Love for protocols and technical advice; and Paul Cullen, Joseph Barbi, and members of the Walker lab for helpful feedback on this manuscript.

FUNDING

This work was supported by the National Institutes of Health [R00GM119173 to S.W.]; and start-up funds from the University at Buffalo College of Arts and Sciences.

REFERENCES:

1. Mitchell, S.F., Walker, S.E., Rajagopal, V., Aitken, C.E. and Lorsch, J.R. (2011) Recruiting knotty partners: The roles of translation initiation factors in mRNA recruitment to the eukaryotic ribosome. *Ribosomes: Structure, Function, and Dynamics*, 155-169.
2. Ozes, A.R., Feoktistova, K., Avanzino, B.C. and Fraser, C.S. (2011) Duplex unwinding and ATPase activities of the DEAD-box helicase eIF4A are coupled by eIF4G and eIF4B. *J Mol Biol*, **412**, 674-687.
3. Rozovsky, N., Butterworth, A.C. and Moore, M.J. (2008) Interactions between eIF4AI and its accessory factors eIF4B and eIF4H. *RNA*, **14**, 2136-2148.
4. Dmitriev, S.E., Terenin, I.M., Dunaevsky, Y.E., Merrick, W.C. and Shatsky, I.N. (2003) Assembly of 48S translation initiation complexes from purified components with mRNAs that have some base pairing within their 5' untranslated regions. *Mol Cell Biol*, **23**, 8925-8933.
5. Mitchell, S.F., Walker, S.E., Algire, M.A., Park, E.H., Hinnebusch, A.G. and Lorsch, J.R. (2010) The 5'-7-methylguanosine cap on eukaryotic mRNAs serves both to stimulate canonical translation initiation and to block an alternative pathway. *Mol Cell*, **39**, 950-962.
6. Sen, N.D., Zhou, F.J., Harris, M.S., Ingolia, N.T. and Hinnebusch, A.G. (2016) eIF4B stimulates translation of long mRNAs with structured 5 ' UTRs and low closed-loop potential but weak dependence on eIF4G. *P Natl Acad Sci USA*, **113**, 10464-10472.
7. Coppolecchia, R., Buser, P., Stotz, A. and Linder, P. (1993) A new yeast translation initiation factor suppresses a mutation in the eIF-4A RNA helicase. *EMBO J*, **12**, 4005-4011.
8. Altmann, M., Muller, P.P., Wittmer, B., Ruchti, F., Lanker, S. and Trachsel, H. (1993) A Saccharomyces cerevisiae homologue of mammalian translation initiation factor 4B contributes to RNA helicase activity. *EMBO J*, **12**, 3997-4003.
9. Andreou, A.Z. and Klostermeier, D. (2014) eIF4B and eIF4G jointly stimulate eIF4A ATPase and unwinding activities by modulation of the eIF4A conformational cycle. *J Mol Biol*, **426**, 51-61.
10. Rogers, G.W., Jr., Richter, N.J., Lima, W.F. and Merrick, W.C. (2001) Modulation of the helicase activity of eIF4A by eIF4B, eIF4H, and eIF4F. *J Biol Chem*, **276**, 30914-30922.
11. Sen, N.D., Zhou, F., Ingolia, N.T. and Hinnebusch, A.G. (2015) Genome-wide analysis of translational efficiency reveals distinct but overlapping functions of yeast DEAD-box RNA helicases Ded1 and eIF4A. *Genome Res*, **25**, 1196-1205.
12. Park, E.H., Zhang, F., Warringer, J., Sunnerhagen, P. and Hinnebusch, A.G. (2011) Depletion of eIF4G from yeast cells narrows the range of translational efficiencies genome-wide. *BMC Genomics*, **12**, 68.
13. Walker, S.E., Zhou, F., Mitchell, S.F., Larson, V.S., Valasek, L., Hinnebusch, A.G. and Lorsch, J.R. (2013) Yeast eIF4B binds to the head of the 40S ribosomal subunit and promotes mRNA recruitment through its N-terminal and internal repeat domains. *RNA*, **19**, 191-207.
14. Fleming, K., Ghuman, J., Yuan, X., Simpson, P., Szendroi, A., Matthews, S. and Curry, S. (2003) Solution structure and RNA interactions of the RNA recognition motif from eukaryotic translation initiation factor 4B. *Biochemistry*, **42**, 8966-8975.
15. Xue, B., Dunbrack, R.L., Williams, R.W., Dunker, A.K. and Uversky, V.N. (2010) PONDR-FIT: a meta-predictor of intrinsically disordered amino acids. *Biochim Biophys Acta*, **1804**, 996-1010.

16. Niederberger, N., Trachsel, H. and Altmann, M. (1998) The RNA recognition motif of yeast translation initiation factor Tif3/eIF4B is required but not sufficient for RNA strand-exchange and translational activity. *RNA*, **4**, 1259-1267.
17. Zhou, F.J., Walker, S.E., Mitchell, S.F., Lorsch, J.R. and Hinnebusch, A.G. (2014) Identification and characterization of functionally critical, conserved motifs in the internal repeats and N-terminal domain of yeast translation initiation factor 4B (yeIF4B). *Journal of Biological Chemistry*, **289**, 11860-11860.
18. Andreou, A.Z., Harms, U. and Klostermeier, D. (2017) eIF4B stimulates eIF4A ATPase and unwinding activities by direct interaction through its 7-repeats region. *RNA Biol*, **14**, 113-123.
19. Park, E.H., Walker, S.E., Zhou, F., Lee, J.M., Rajagopal, V., Lorsch, J.R. and Hinnebusch, A.G. (2013) Yeast eukaryotic initiation factor 4B (eIF4B) enhances complex assembly between eIF4A and eIF4G in vivo. *J Biol Chem*, **288**, 2340-2354.
20. Altmann, M., Wittmer, B., Methot, N., Sonenberg, N. and Trachsel, H. (1995) The Saccharomyces cerevisiae translation initiation factor Tif3 and its mammalian homologue, eIF-4B, have RNA annealing activity. *EMBO J*, **14**, 3820-3827.
21. Mulleder, M., Capuano, F., Pir, P., Christen, S., Sauer, U., Oliver, S.G. and Ralser, M. (2012) A prototrophic deletion mutant collection for yeast metabolomics and systems biology. *Nat Biotechnol*, **30**, 1176-1178.
22. Bochner, B.R., Gadzinski, P. and Panomitros, E. (2001) Phenotype microarrays for high-throughput phenotypic testing and assay of gene function. *Genome Res*, **11**, 1246-1255.
23. Lee, B., Udagawa, T., Singh, C.R. and Asano, K. (2007) Yeast phenotypic assays on translational control. *Methods Enzymol*, **429**, 105-137.
24. Ingolia, N.T., Ghaemmaghami, S., Newman, J.R. and Weissman, J.S. (2009) Genome-wide analysis in vivo of translation with nucleotide resolution using ribosome profiling. *Science*, **324**, 218-223.
25. McGlincy, N.J. and Ingolia, N.T. (2017) Transcriptome-wide measurement of translation by ribosome profiling. *Methods*, **126**, 112-129.
26. Guydosh, N.R. and Green, R. (2014) Dom34 rescues ribosomes in 3' untranslated regions. *Cell*, **156**, 950-962.
27. Michel, A.M., Mullan, J.P., Velayudhan, V., O'Connor, P.B., Donohue, C.A. and Baranov, P.V. (2016) RiboGalaxy: A browser based platform for the alignment, analysis and visualization of ribosome profiling data. *RNA Biol*, **13**, 316-319.
28. Martin, M. (2011) Cutadapt Removes Adapter Sequences From High-Throughput Sequencing Reads. *EMBnet.journal*, **17**, 10-12.
29. Langmead, B., Trapnell, C., Pop, M. and Salzberg, S.L. (2009) Ultrafast and memory-efficient alignment of short DNA sequences to the human genome. *Genome Biol*, **10**, R25.
30. Love, M.I., Huber, W. and Anders, S. (2014) Moderated estimation of fold change and dispersion for RNA-seq data with DESeq2. *Genome Biol*, **15**, 550.
31. Thompson, M.K., Rojas-Duran, M.F., Gangaramani, P. and Gilbert, W.V. (2016) The ribosomal protein Asc1/RACK1 is required for efficient translation of short mRNAs. *Elife*, **5**.
32. Lambert, D. and Draper, D.E. (2012) Denaturation of RNA secondary and tertiary structure by urea: simple unfolded state models and free energy parameters account for measured m-values. *Biochemistry*, **51**, 9014-9026.
33. Necas, O. and Svoboda, A. (1973) Effect of urea on the plasma membrane particles in yeast cells and protoplasts. *Protoplasma*, **77**, 453-466.
34. Cooper, T.G. and Sumrada, R. (1975) Urea transport in Saccharomyces cerevisiae. *J Bacteriol*, **121**, 571-576.
35. Dolan, K., Montgomery, S., Buchheit, B., Didone, L., Wellington, M. and Krysan, D.J. (2009) Antifungal activity of tamoxifen: in vitro and in vivo activities and mechanistic characterization. *Antimicrob Agents Chemother*, **53**, 3337-3346.
36. Kim, J., Oh, J. and Sung, G.H. (2016) Regulation of MAP kinase Hog1 by calmodulin during hyperosmotic stress. *Biochim Biophys Acta*, **1863**, 2551-2559.
37. Kertesz, M., Wan, Y., Mazor, E., Rinn, J.L., Nutter, R.C., Chang, H.Y. and Segal, E. (2010) Genome-wide measurement of RNA secondary structure in yeast. *Nature*, **467**, 103-107.
38. Costello, J., Castelli, L.M., Rowe, W., Kershaw, C.J., Talavera, D., Mohammad-Qureshi, S.S., Sims, P.F.G., Grant, C.M., Pavitt, G.D., Hubbard, S.J. *et al.* (2015) Global mRNA selection mechanisms for translation initiation. *Genome Biol*, **16**.
39. Methot, N., Song, M.S. and Sonenberg, N. (1996) A region rich in aspartic acid, arginine, tyrosine, and glycine (DRYG) mediates eukaryotic initiation factor 4B (eIF4B) self-association and interaction with eIF3. *Mol Cell Biol*, **16**, 5328-5334.

40. Methot, N., Pickett, G., Keene, J.D. and Sonenberg, N. (1996) In vitro RNA selection identifies RNA ligands that specifically bind to eukaryotic translation initiation factor 4B: the role of the RNA remotif. *RNA*, **2**, 38-50.
41. Naranda, T., Strong, W.B., Menaya, J., Fabbri, B.J. and Hershey, J.W. (1994) Two structural domains of initiation factor eIF-4B are involved in binding to RNA. *J Biol Chem*, **269**, 14465-14472.
42. Methot, N., Pause, A., Hershey, J.W. and Sonenberg, N. (1994) The translation initiation factor eIF-4B contains an RNA-binding region that is distinct and independent from its ribonucleoprotein consensus sequence. *Mol Cell Biol*, **14**, 2307-2316.
43. Navarathna, D.H., Das, A., Morschhauser, J., Nickerson, K.W. and Roberts, D.D. (2011) Dur3 is the major urea transporter in Candida albicans and is co-regulated with the urea amidolyase Dur1,2. *Microbiology*, **157**, 270-279.
44. Navarathna, D.H., Harris, S.D., Roberts, D.D. and Nickerson, K.W. (2010) Evolutionary aspects of urea utilization by fungi. *FEMS Yeast Res*, **10**, 209-213.
45. Ghosh, S., Navarathna, D.H., Roberts, D.D., Cooper, J.T., Atkin, A.L., Petro, T.M. and Nickerson, K.W. (2009) Arginine-induced germ tube formation in Candida albicans is essential for escape from murine macrophage line RAW 264.7. *Infect Immun*, **77**, 1596-1605.

TABLE AND FIGURE LEGENDS

Table 1: Gene Ontology analysis for genes with decreased translational efficiency in Δ*ntd* compared to WT in the presence of urea

GO Term	p-Value
Transferase activity, transferring hexosyl groups [GO:0016758]	1.62E-06
Endomembrane system [GO:0012505]	1.44E-05
Transferase activity, transferring glycosyl groups [GO:0016757]	2.22E-04
Protein glycosylation [GO:0006486]	3.76E-04
Macromolecule glycosylation [GO:0043413]	3.76E-04
Mannosylation [GO:0097502]	5.19E-04
Glycoprotein biosynthetic process [GO:0009101]	8.19E-04
Cellular bud [GO:0005933]	1.55E-03
Protein N-linked glycosylation [GO:0006487]	1.91E-03
Glycosylation [GO:0070085]	2.40E-03
Glycoprotein metabolic process [GO:0009100]	2.85E-03
Cell periphery [GO:0071944]	4.09E-03
Golgi cisterna [GO:0031985]	4.70E-03
Cell part [GO:0044464]	8.14E-03
Cell [GO:0005623]	8.81E-03
Protein O-linked glycosylation [GO:0006493]	1.98E-02
Golgi stack [GO:0005795]	2.26E-02
Mannosyltransferase activity [GO:0000030]	3.04E-02
Organelle subcompartment [GO:0031984]	3.65E-02
Membrane part [GO:0044425]	4.69E-02

Figure 1. The N-terminal domain of eIF4B binds the ribosome and promotes translation in a prototrophic yeast strain. A. Schematic of eIF4B functional domains in WT strain (upper) and the NTD deletion mutant construct (lower). **B-C**. Association of eIF4B with the ribosome in WT (**B**) or NTD deletion (**C**) strains assayed by Western blotting of fractions (bottom) isolated from clarified lysates resolved by velocity sedimentation through 10%-50% sucrose gradients (top, representative polysome profiles), while scanning at 254 nm.

Figure 2. eIF4B binding to the 40S promotes resistance to stressors that challenge cellular integrity through changes in translation. A. Heatmap of average height differences for cellular fitness between the NTD deletion mutant (green) and WT (red) under 1440 metabolic and chemical conditions as assayed by Phenotype microarray, which includes seven panels in 15 96-well plates: 1. Carbon Sources; 2. Nitrogen Sources; 3. Phosphorus and Sulfur Sources; 4. Nutrient Supplements; 5. Peptide Nitrogen Sources; 6. Osmolytes; 7. pH; and 8. Chemical Sensitivity. Wells containing 2%, 3%, and 4% urea are outlined by a black box. 3% Urea gave the largest difference in WT and Δ*ntd* fitness. **B.** Growth curves of WT (black) and the NTD deletion mutant (red) grown with 0% (circles), 2% (squares), or 3% urea (triangles). Results from biological triplicates ± SEM are shown. **C**. Relative change in polysome to monosome (P:M) ratio upon exposure to urea was determined as in B and C in the presence and absence of 3% urea. Biological triplicates ± SEM are shown with P values from Student's t test indicated (*$P < 0.05$). **D**. eIF4B levels in WT or NTD deletion mutant grown with 0, 2%, or 3% urea in Synthetic Dextrose media.

Figure 3. The NTD of eIF4B promotes translation of mRNAs encoding proteins associated with the membrane and cell wall. A-C. Comparison of Log_2 values for changes in RNAseq (**A**), Riboseq (**B)**, or TE (**C**, Translation efficiency) in response to 3% urea for WT are plotted vs. the Log_2 values for changes observed in the NTD deletion mutant for each of the 4070 genes with measurable expression in each group. Pearson correlation coefficients are shown. **D-F**. Overlap of urea-dependent genes exhibiting 1.5-fold or greater increase in RNAseq (**D**), Riboseq (**E**), or TE (**F**) for WT and Δ*ntd*. **G**. Gene ontology analysis for mRNAs with increased TE in WT in response to urea.

Figure 4. Comparison of PARS (Parallel analysis of RNA structure) scores indicates a higher propensity for secondary structure in the 5'UTRs of mRNAs that are dependent on the NTD for translation, and in mRNAs encoding proteins trafficked through the ER and Golgi. A. Schematic showing 5'-UTR and CDS intervals for cumulative PARS scores. The sum of scores for all 5'-UTR nucleotides (5'UTR PARS); for the first 30 nucleotides (First 30 PARS); for 30 nucleotides surrounding the start codon (Start 30 PARS); and for nucleotides within the ORF, from +1 to +30 (Plus15), +16 to +45 (Plus30), +31 to +60 (Plus45), +46 to +75 (Plus60), and +61 to +90 (Plus75). **B-C.** The mean PARS scores (calculated from data reported in reference (37)) for indicated cumulative regions (**B**), or for

individual nucleotides in the 5'UTR (**C**) are indicated for all yeast mRNAs with available PARS scores (gray, n=2679); mRNAs with decreased TE (≥1.5-fold) in Δ*ntd* relative to WT in media lacking urea (red, n=138); and for mRNAs with decreased TE in Δ*ntd* relative to WT in 3% urea (navy, n=156). **D**. Average length of 5'-UTR for the indicated sets of mRNAs. **E-G**. Averaged cumulative (E) and average 5'UTR nucleotide (G) PARS scores and 5'UTR lengths (F) for all genes associated with indicated gene ontology categories: intrinsic component of membrane (orange, n=1360), transferase (blue, n=86), endomembrane system (purple, n=1098), glycosylation (green, n=87), or mannosylation (yellow, n=46) for each 5'-UTR or CDS interval described in **A-D**, with P values from Student's t test indicated (*P < 0.05).

Figure 5. The NTD of eIF4B promotes translation of mRNAs with structured 5'-UTRs that reinforce the cellular periphery and allow a robust cellular response to urea. WT eIF4B promotes PIC loading and scanning of all mRNAs. Deletion of the NTD of eIF4B reduces translation of mRNAs with long structured 5'UTRs, indicating eIF4B promotes ribosome loading and scanning while bound to the PIC. Translation of these highly structured mRNAs are required to reconfigure the membrane proteome in response to stressors, providing urea resistance.

Figure 1

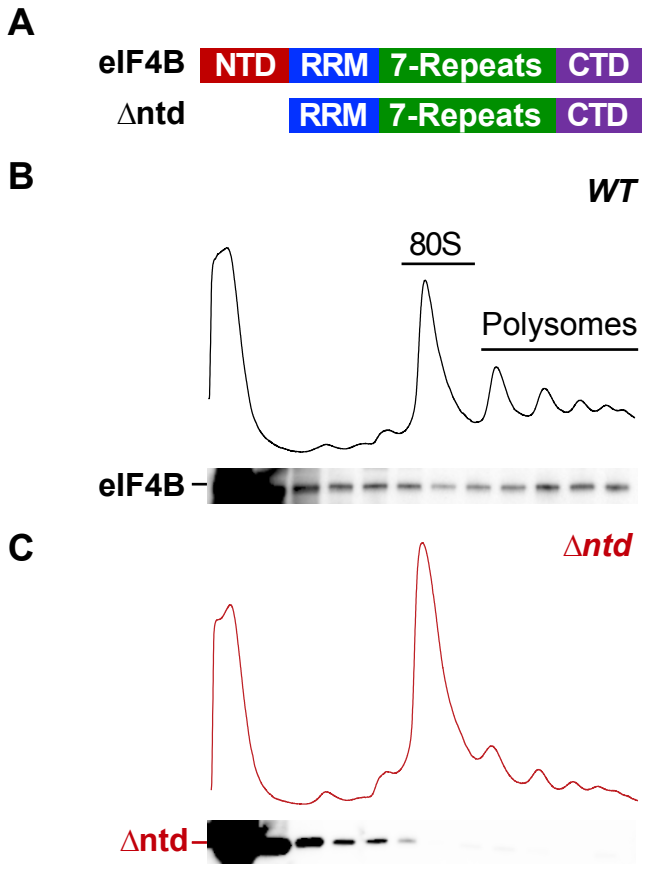
A
eIF4B
NTD
RRM
7-Repeats
CTD
Δntd
RRM
7-Repeats
CTD
B
WT
80S
Polysomes
eIF4B
C
Δntd
Δntd

Figure 2

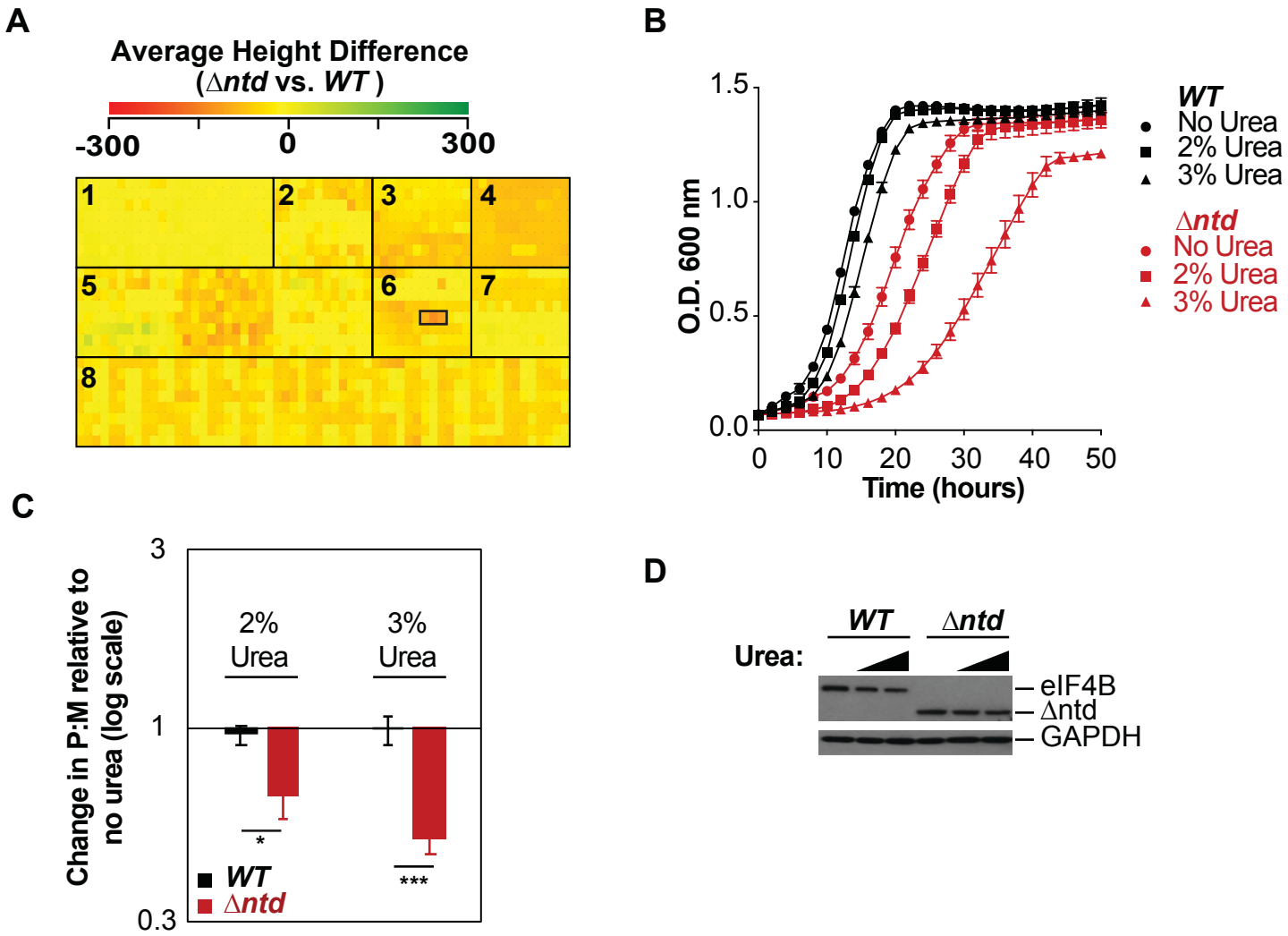
A
Average Height Difference
(Δntd vs. WT)
-300
0
300
1
2
3
4
5
6
7
8
B
1.5
1.0
0.5
0.0
O.D. 600 nm
0
10
20
30
40
50
Time (hours)
WT
No Urea
2% Urea
3% Urea
Δntd
No Urea
2% Urea
3% Urea
C
3
1
0.3
Change in P:M relative to no urea (log scale)
2% Urea
3% Urea
*
***
WT
Δntd
D
WT
Δntd
Urea:
eIF4B
Δntd
GAPDH

Figure 3

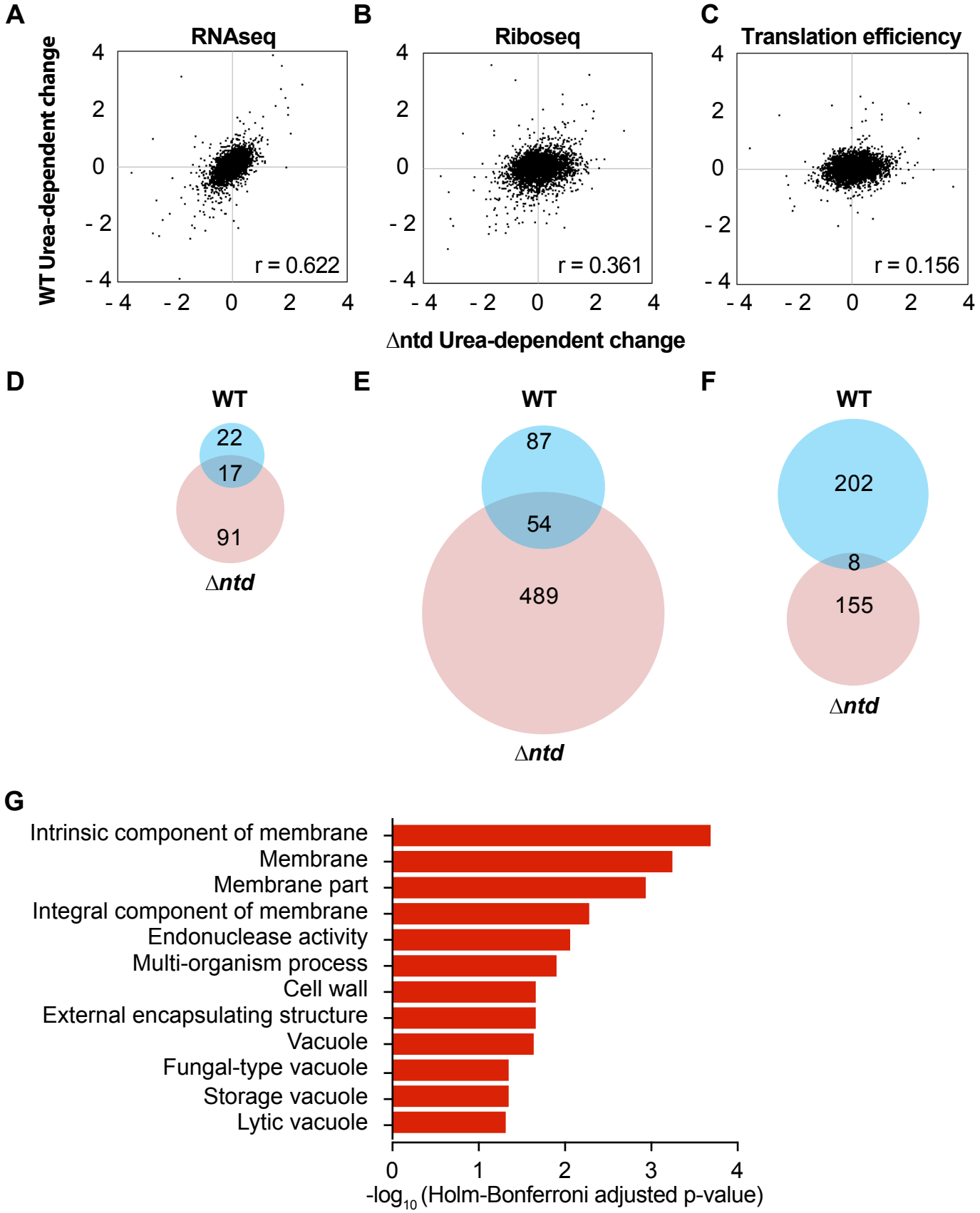
A
RNAseq
r = 0.622
B
Riboseq
r = 0.361
C
Translation efficiency
r = 0.156
WT Urea-dependent change
Δntd Urea-dependent change
D
WT
22
17
91
Δntd
E
WT
87
54
489
Δntd
F
WT
202
8
155
Δntd
G
Intrinsic component of membrane
Membrane
Membrane part
Integral component of membrane
Endonuclease activity
Multi-organism process
Cell wall
External encapsulating structure
Vacuole
Fungal-type vacuole
Storage vacuole
Lytic vacuole
-log10 (Holm-Bonferroni adjusted p-value)

Figure 4

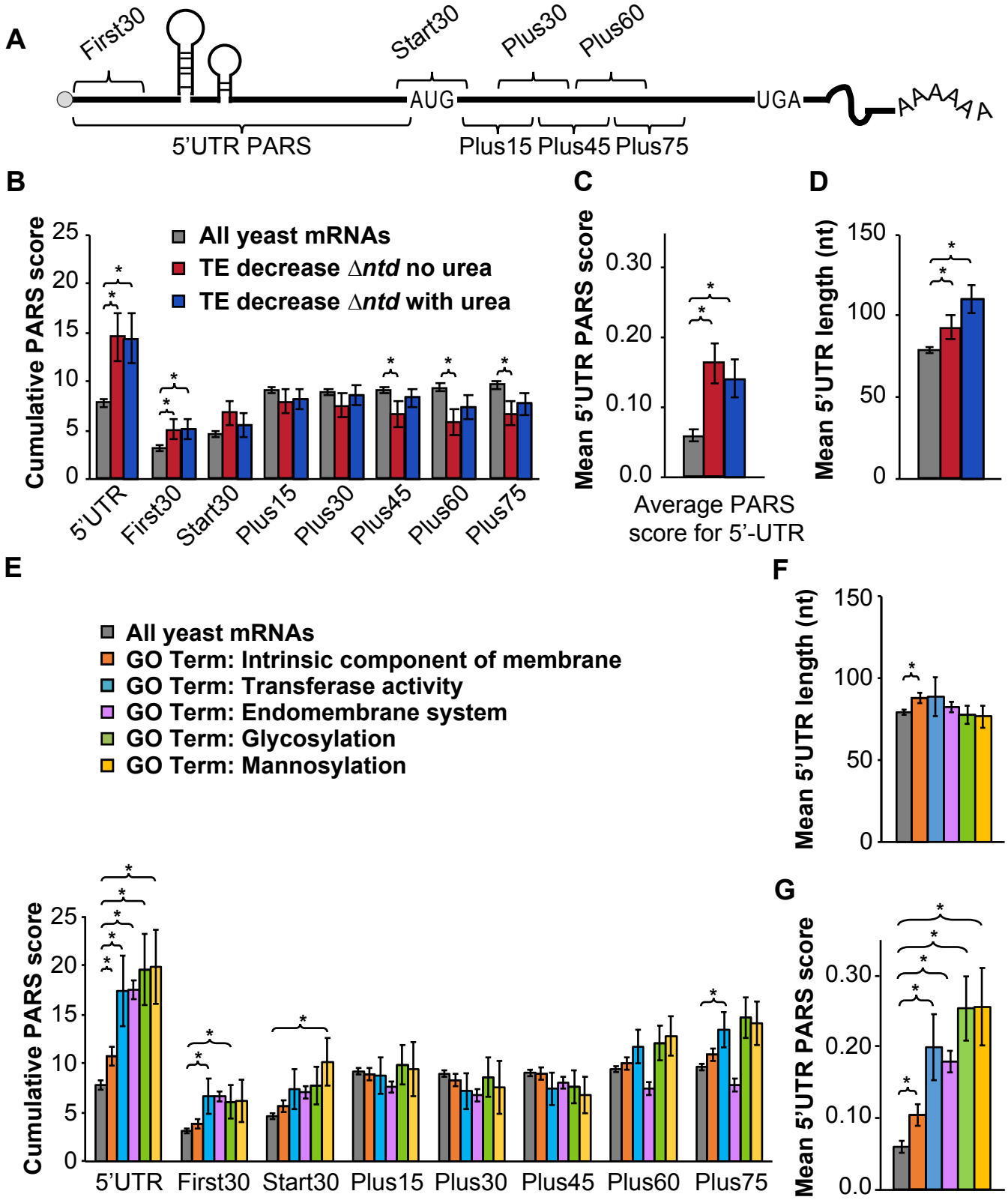
A
First30
Start30
Plus30
Plus60
AUG
UGA
AAAAAAA
5'UTR PARS
Plus15 Plus45 Plus75
B
Cumulative PARS score
All yeast mRNAs
TE decrease Δntd no urea
TE decrease Δntd with urea
5'UTR
First30
Start30
Plus15
Plus30
Plus45
Plus60
Plus75
C
Mean 5'UTR PARS score
Average PARS score for 5'-UTR
D
Mean 5'UTR length (nt)
E
All yeast mRNAs
GO Term: Intrinsic component of membrane
GO Term: Transferase activity
GO Term: Endomembrane system
GO Term: Glycosylation
GO Term: Mannosylation
F
Mean 5'UTR length (nt)
G
Mean 5'UTR PARS score

Figure 5

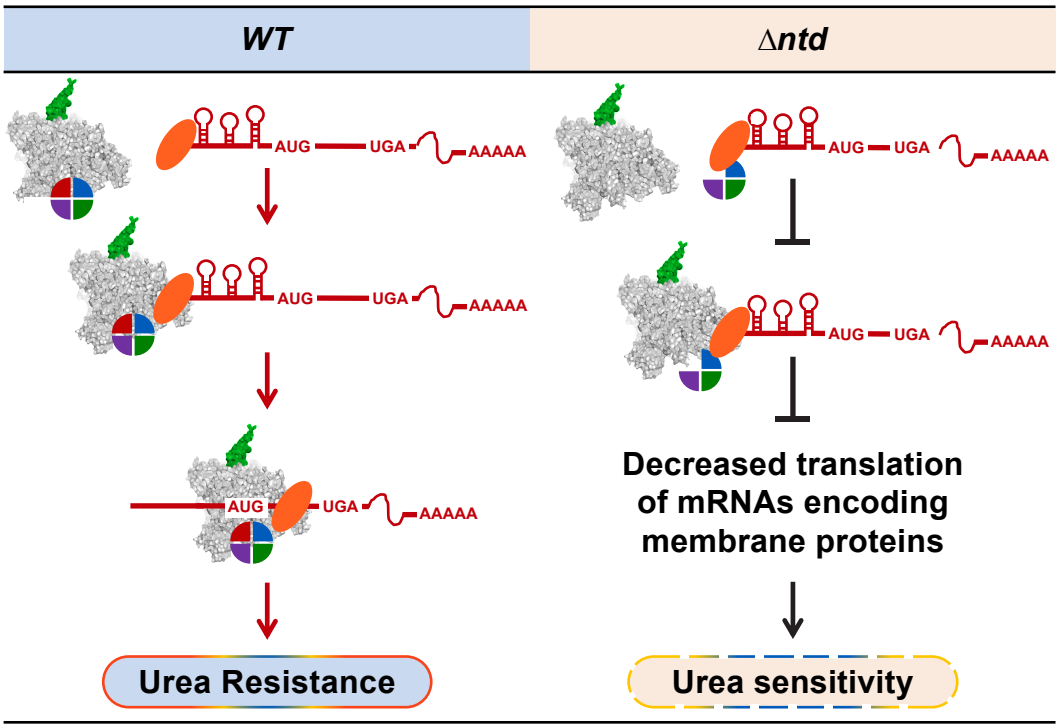
WT
Δntd
AUG
UGA
AAAAA
Decreased translation of mRNAs encoding membrane proteins
Urea Resistance
Urea sensitivity